Transcriptomic profiles of the ovaries from piglets neonatally exposed to 4-*tert*-octylphenol

Katarzyna Knapczyk-Stwora [a], Anna Nynca [b], Renata E. Ciereszko [b, c], Lukasz Paukszto [d], Jan P. Jastrzebski [d], Elzbieta Czaja [a], Patrycja Witek [a], Marek Koziorowski [e], Maria Slomczynska [a, *]

[a] *Department of Endocrinology, Institute of Zoology and Biomedical Research, Faculty of Biology, Jagiellonian University, Gronostajowa 9, 30-387, Krakow, Poland*
[b] *Laboratory of Molecular Diagnostics, Faculty of Biology and Biotechnology, University of Warmia and Mazury, Prawochenskiego 5, 10-720, Olsztyn, Poland*
[c] *Department of Animal Anatomy and Physiology, Faculty of Biology and Biotechnology, University of Warmia and Mazury, Oczapowskiego 1A, 10-719, Olsztyn, Poland*
[d] *Department of Plant Physiology, Genetics and Biotechnology, Faculty of Biology and Biotechnology, University of Warmia and Mazury, Oczapowskiego 1A, 10-719, Olsztyn, Poland*
[e] *Department of Physiology and Reproduction of Animals, Institute of Biotechnology, University of Rzeszow, Werynia 502, 36-100, Kolbuszowa, Poland*

ARTICLE INFO

ABSTRACT

The environmental pollutants with hormonal activities may influence steroid-mediated processes in neonatal ovaries and increase the incidence of reproductive disorders. The aim of the current study was to examine effects of 4-*tert*-octylphenol (OP), a non-ionic surfactant widely used in a variety of industrial applications which has been reported to mimic the 17β-estradiol activity, on the expression of protein-coding (mRNAs) and long non-coding (lncRNAs) transcripts in neonatal ovaries of the pig. By employing RNA-Seq we aimed to gain insights into regulatory networks underlying the OP effects on the follicular development in pigs. Piglets were injected (sc) daily with OP (100 mg/kg bw) or corn oil (controls) between postnatal Days 1 and 10 (n = 3/group). Ovaries were excised from the 11-day-old piglets and total cellular RNA was isolated and sequenced. Two hundred three differentially expressed genes (DEGs; P-adjusted < 0.05 and log₂ fold change ≥1.0) and 23 differentially expressed lncRNAs (DELs; P-adjusted < 0.05 and log₂ fold change ≥ 1.0) were identified in OP-treated piglet ovaries. The DEGs were assigned to Gene Ontology terms, covering biological processes, molecular functions and cellular components, which linked the DEGs to functions associated with movement of cell or subcellular component, regulation of plasma membrane bounded cell projection assembly as well as hydrolase and endopeptidase activity. In addition, STRING analysis demonstrated the strongest interactions between genes related to negative regulation of endopeptidase activity. Some correlations between DEGs and DELs were also found, revealing that the OP action on the ovary may be partially executed *via* the changes in the lncRNA expression. These results suggest that neonatal exposure of pigs to OP induces changes in the ovarian transcriptomic profile associated with genes encoding serine protease inhibitors and involved in steroid synthesis as well as genes linked to intracellular and membrane transport. We suggest that the changes in the mRNA and lncRNA expression in the ovaries of OP-treated piglets may disturb ovarian cellular function, including steroidogenesis, proliferation and apoptosis.

1. Introduction

Development of a healthy ovary during fetal/neonatal life is essential for future reproductive success. In pigs, folliculogenesis begins during fetal life but the ovarian follicular reserve is established during the neonatal period around postnatal day (PD) 25 [1]. Female fertility is determined by the size of the follicular reserve and its depletion rate. The excessive follicular activation and/or atresia may lead to an early depletion of the follicular reserve resulting in infertility [2]. The ovarian follicle formation and growth is a complex and tightly regulated process governed by many extra- and intra-follicular factors, including steroid hormones [3].

* Corresponding author.
E-mail address: maria.slomczynska@uj.edu.pl (M. Slomczynska).

It is generally recognized that abnormal development of reproductive system and an increased incidence of reproductive disorders may result from extensive usage of endocrine active chemicals (EACs). Animals during the fetal and neonatal periods are very susceptible to EACs and even a low-dose exposure may produce adverse effects due to immature reproductive and immune systems [4]. EACs displaying estrogenic, antiestrogenic, androgenic and antiandrogenic activities may disrupt the proper action of endogenous hormones [5]. EACs identified as environmental estrogens include phytoestrogens, polycyclic aromatic hydrocarbons (polychlorinated biphenyls, furans and dioxins) and some alkylphenolic compounds (e.g., 4-*tert*-octylphenol and nonylphenol) [6]. 4-*tert*-octylphenol (OP) is widely used in a variety of industrial applications including the production of pesticides, herbicides, glass fiber, rubber and polystyrene products as well as detergents, as emulsifiers in water-based paints [7]. This alkylphenol has been reported to bind to estrogen receptors (ERs) and to mimic the effects of 17β-estradiol (E_2) [8]. Although OP displays rather low estrogenic potency (>1000 times less potent than E_2), *in vitro* studies using human breast cancer cells (MCF-7 and ZR-75-1) demonstrated its ability to induce estrogen-dependent biological responses such as cell growth and stimulation the transcriptional activity of estrogen receptor [8]. Moreover, *in vivo* studies showed that maternally or neonatally injected OP caused adverse effects on male and female reproductive tracts in adult rats [9,10]. In male rats, OP treatment during fetal period revealed abnormalities in the histology of the testis and epididymis, induced atrophy of prostate glands tubules, and affected sperm structure [9]. In female rats, the neonatal exposure to OP altered the hormonal environment in the early period of the reproductive tract development. The hormonal changes led to persistent estrus, anovulation, polycystic ovaries and affected proliferation of uterine tissues [10]. Bøgh et al. [7] reported a transgenerational effects of intrauterine exposure to OP in pigs. These effects included an acceleration of the puberty onset and a reduced litter size.

Previously, we showed that neonatal exposure to testosterone propionate, flutamide, ICI 182,780, methoxychlor and OP affected early folliculogenesis in 11-day-old piglets [11]. OP increased the formation of follicles and their initial recruitment which potentially might be responsible for the acceleration of folliculogenesis and consequent primary ovarian insufficiency in adulthood [11]. The results of our recent RNA-sequencing (RNA-Seq) study demonstrated that neonatal exposure of piglets to antiandrogen flutamide altered the expression of genes involved in ovarian cell proliferation, steroidogenesis and oocyte fertilization [12]. Thus, environmental pollutants with hormonal activities may influence steroid-mediated processes within neonatal ovaries in pigs. However, the mechanism of OP action in the porcine neonatal ovary is not fully recognized.

To unveil the molecular basis of this mechanism, RNA-Seq was used in the current study to analyze the expression of protein-coding (mRNAs) and long non-coding (lncRNAs) transcripts in the ovaries of piglets neonatally exposed to OP. lncRNAs were recently reported to be involved in the regulation of gene expression, mRNA processing and stability as well as protein stability and cellular protein localization [13,14]. To learn how OP affects the expression of both mRNA and lncRNA transcripts will help to better understand the molecular mechanisms underlying the OP effects on the follicular development.

2. Material and methods

2.1. Animals and tissue sampling

Six pig neonates (Large White × Polish Landrace) originating from different litters were randomly allotted into two experimental groups i.e., control (CTR; n = 3 piglets) and OP-treated (OP; n = 3 piglets) group. The latter group received injections of OP (100 mg/kg bw, in 1 ml of corn oil; Sigma-Aldrich, St. Louis, MO, USA). Piglets from the control group were given 1 ml of corn oil only. The animals were subcutaneously (sc) injected daily between PD1 and PD10. This dose was chosen on the basis of our previous experiments [15,16] as well as literature review [10,17]. During the entire experiment all piglets were housed together with theirs mothers and siblings. The ovaries of each individual of the two groups were excised one day after the last injection (PD11), snap-frozen in liquid nitrogen and stored at −80 °C until RNA extraction. All procedures were performed by a veterinarian. The use of animals was approved by the Local Ethics Committee at the Jagiellonian University in Krakow, Poland (approval number 150/2013, 122/2014 and 123/2014).

2.2. Total RNA extraction, quantification and integrity testing

Total RNA from the collected ovaries was extracted using TRI Reagent (Ambion, Austin, TX, USA) following the manufacturer's protocol. Concentration and purity of the total RNA samples were measured spectrophotometrically (NanoVue Plus, GE Healthcare, Little Chalfont, UK). RNA integrity was assessed with an Agilent 2100 Bioanalyzer and the RNA 6000 Nano LabChip kit (Agilent Technologies, Santa Clara, CA, USA). RNA integrity number (RIN) values for all samples used for RNA-Seq were ≥8.

2.3. Construction and sequencing of illumina cDNA libraries

Depleted RNA (400 ng) obtained from total RNA was used to construct cDNA libraries (TruSeq Stranded mRNA Sample Prep Kit; Illumina, San Diego, CA, USA) [12]. First and second cDNA strands were synthesized after RNA purification and fragmentation. Next steps included 3′ ends adenylation, adapter ligation and library amplification (PCR). Library profiles were estimated using the DNA High Sensitivity Lab- Chip kit on the 2100 Bioanalyzer (Agilent Technologies). Libraries were then sequenced on a NextSeq500 instrument (Illumina) with 150 paired-end sequencing (Sequencing No. 1 - Seq 1). Since the obtained data showed that the transcriptome of one control ovary (CTR3) differed distinctly from other control ovaries, the RNA sequencing of all samples was repeated to eliminate errors of the sequencing procedure (Sequencing No. 2 − Seq 2). In consequence, we have analyzed transcripts from the ovaries of three control (CTR1, CTR2, CTR3) and three 4-*tert*-octylphenol-treated (OP1, OP2, OP3) piglets, where each piglet represented a biological sample. Each biological sample, in turn, was represented by two technical samples originating from Seq 1 (CTR1a, CRT2a, CTR3a, OP1a, OP2a, OP3a) and Seq 2 (CTR1b, CRT2b, CTR3b, OP1b, OP2b, OP3b). Results of the Seq 2 confirmed that the CTR3 sample displayed a different transcriptome profile, and this sample was excluded from further analysis. Thus, the following analysis of the transcript expression level was performed on four control samples (two biological samples) and six 4-*tert*-octylphenol-treated samples (three biological samples).

2.4. Bioinformatic analysis of gene expression

The raw sequenced data (reads) in FASTQ format were deposited in NCBI-SRA database under the BioProject accession number PRJNA413646. The samples are available as the BioSamples records under the accession numbers: SAMN07806805, SAMN07806806, SAMN07806807, SAMN07806808 (controls) and SAMN07806829, SAMN07806830, SAMN07806831, SAMN07806832, SAMN07806833, SAMN07806834 (OP-treated). The reads were trimmed using

the Trimmomatic v.0.39 tool [18], and sequences of average PHRED30 score lower than 20 were removed. The read quality was evaluated using FastQC v 11.08 program (http://www.bioinformatics. babraham.ac.uk/projects/fastqc/). The good quality fragments were mapped to the porcine genome (Sus_scrofa.Sscrofa11.1; Ensembl data-base with annotation version 11.1.91) using STAR v2.4.0.1 [19]. The StringTie 1.0.4 [20,21] and Cufflinks v2.2.1 [22] tools were used to determine the expression level of all transcripts.

The differential expression analysis of control (CTR1 and CTR2) and OP-treated (OP1, OP2 and OP3) samples was done with Cuffdiff (https://doi.org/10.1038/nbt.2450) and DESeq2 [23] methods using Bioconductor [24,25] of R statistical software. The differentially expressed genes (DEGs) were identified as genes of P-adjusted < 0.05 and absolute normalized ($\log_2$) fold change higher or equal to 1 in both statistical methods.

2.5. Functional enrichment analysis

The Gene Ontology (GO) enrichment of DEGs into three categories (molecular function, cellular component and biological process) was performed using g:Profiler tool [26] with P-value threshold at the level of 0.05. Moreover, the Bioinformatics Database STRING 10.5 (Search Tool for the Retrieval of Interacting Genes, http://string-db.org) was used to investigate the possible gene association networks between DEGs [27]. The searching criteria were based on the co-occurrence of genes/proteins in scientific texts (text mining), co-expression and experimentally observed interactions. This analysis generated gene/protein interaction networks, where strength of the interaction score was set as 0.7. In addition, Kyoto Encyclopedia of Genes and Genomes (KEGG) analysis (P < 0.05) was performed to assign the OP-affected DEGs to the ovarian steroidogenesis pathway.

2.6. Identification, characterization and analysis of lncRNAs

ENSEMBL/GENCODE database was used to identify known lncRNAs. To identify putative novel lncRNAs, the customized pipeline [12,28] was performed (Fig. 6). The main steps of the pipeline were: 1) removing sequences shorter than 200 nt and those having only one exon, 2) removing all known protein-coding transcripts and 3) removing transcripts with a protein-coding potential. The FPKM (fragments per kilobase of transcript per millions fragments sequenced) values for lncRNA transcripts were calculated using the Cuffnorm (version 2.2.1) in the Cufflinks package. The differences in expression level of the identified lncRNAs (differentially expressed lncRNAs [DELs]) were calculated in the same way as DEGs. The correlation between DELs and DEGs was calculated based on the Pearson method.

2.7. Real-time PCR

To verify the RNA-Seq results, four up- and down-regulated DEGs and one DEL were selected for quantitative real-time PCR analysis (qRT-PCR). The same RNA samples were used as the template for RNA-Seq and qRT-PCR. One 1 μg of RNA was reverse-transcribed using a High-Capacity cDNA Reverse Transcription Kit (Applied Biosystems, Foster City, CA, USA) according to the manufacturer's protocol. The reaction was performed in a Veriti Thermal Cycler (Applied Biosystems). Real time PCR was performed with the StepOneTM Real-Time PCR System (Applied Biosystems) using TaqMan Gene Expression Master Mix (Applied Biosystems) and porcine-specific TaqMan Gene Expression Assays (Applied Biosystems) for claudin 1 (CLDN1; Ss04329019_s1), cytochrome P450 11A1 (CYP11A1; Ss03384849_u1), serpin A1 (SERPINA1; Ss03394873_m1), serpin A6 (SERPINA6; Ss03392373_m1), and lncRNA - TCONS_00036 806 (Custom Assay

APGZHGF; primer sequences: forward: GGCAGCCTTTTGTTTCCTTA-GAG, reverse: GCTCATTTCAAAGGATACCCATGTG; probe sequence: CTCTAGCATTCATTCTTTTTCT) with endogenous control for glyceraldehyde-3-phosphate dehydrogenase (GAPDH, Ss03373286_u1) following manufacturers' instructions. Each assay was performed in triplicate and non-template control was included in each run. The relative mRNA expression level was calculated using the real-time PCR Miner algorithm [29], which calculates real-time PCR expression values using parameters such as reaction efficiency and the fractional cycle number at the threshold (Ct). Data obtained for CLDN1, CYP11A1, SERPINA1, SERPINA6, and TCONS_00036 806 were normalized to those of obtained for GAPDH and expressed as the mean ± SEM. The nonparametric Mann-Whitney U test was used to determine significant differences between the control and OP-treated group. Differences were considered statistically significant at the 95% confidence level (P < 0.05).

3. Results

3.1. The effects of OP on the mRNA expression profile in porcine neonate ovaries

Sequencing of mRNA isolated from porcine neonatal ovaries produced from 23,817,088 to 33,222,782 raw reads per sample. After rejecting low quality reads (PHRED<20), the remaining reads (21,954,606—31,474,601; 87.0—96.6% per sample) were mapped to the annotated whole porcine genome (Sus_scrofa.Sscrofa11.1). On average 88.4% reads aligned to the genome were mapped to a unique location. The total number of transcripts identified in piglet ovaries ranged from 32,931 to 36,654 per ovary. The summary of data obtained from RNA-Seq of porcine neonatal ovaries is presented in Table 1. The analysis of distance matrices revealed a high level of similarity between biological replicates of the control samples as well as between replicates of the OP-treated samples. Both sequencings produced similar effects (Fig. 1A and B). Distribution of transcripts, in relation to expression profiles (MA plot and volcano plot) in the ovaries of porcine neonates treated with OP are visualized in Fig. 2.

A total of 203 DEGs were determined in the current study. We identified 169 down- and 34 up-regulated DEGs in neonate ovaries after the OP treatment. The expression profile of all DEGs is presented in Fig. 3. The $\log_2$FC values for DEGs ranged from −5.85 (MAP3K19, mitogen-activated protein kinase kinase kinase 19) to 2.97 (CDH12, cadherin 12) (see Supplementary Table 1).

3.2. Functional classification of the OP-affected genes

To discover possible functions of DEGs identified in the ovaries of OP-treated porcine neonates, the genes were classified into three main categories ("biological process", "molecular function" and "cellular component") according to GO database (Fig. 4A, Suppl. Tab. 2). The DEGs classified into "biological process" were mainly annotated to processes included "movement of cell or subcellular component" (32 genes), "negative regulation of hydrolase activity" (13 genes), "microtubule-based movement" (12 genes), "regulation of endopeptidase activity" (12 genes) and "regulation of peptidase activity" (12 genes; Fig. 4A, Suppl. Tab. 2). The "molecular function" GO category encompassed, among others, DEGs annotated to "enzyme inhibitor activity" (12 genes, Fig. 4A, Suppl. Tab. 2). The "cellular component" category linked the DEGs to: "extracellular region" (35 genes), "extracellular space" (29 genes) and "plasma membrane bounded cell projection" (29 genes; Fig. 4A, Suppl. Tab. 2).

A subsequent functional classification of all genes, which expression was significantly affected (P-adjusted < 0.05) by 4-tert-octylphenol, was performed using KEGG database. In the present

Table 1
Summary of RNA-Seq data of ovaries obtained from 4-*tert*-octyphenol-treated porcine neonates.

Sample	CTR1a	CTR1b	CTR2a	CTR2b	OP1a	OP1b	OP2a	OP2b	OP3a	OP3b
Number of row reads	25 218 729	25 684 749	24 265 954	29 793 840	30 143 260	33 222 782	32 996 859	23 817 088	29 635 466	25 422 846
Number of processed reads	22 946 350	24 815 278	22 025 084	28 489 892	27 676 934	31 474 601	28 699 228	21 954 606	26 518 899	23 846 397
% of processed reads	90.99%	96.61%	90.77%	95.62%	91.82%	94.74%	86.98%	92.18%	89.48%	93.80%
Unique reads										
Number of uniquely mapped reads	19 797 905	22 801 129	18 431 707	26 264 253	23 854 507	29 067 049	24 235 014	19 561 013	22 818 465	21 881 140
% of uniquely mapped reads	86.28%	91.88%	83.69%	92.19%	86.19%	92.35%	84.44%	89.10%	86.05%	91.76%
Average mapped length (nt)	177.49	178.23	176.89	178.32	177.55	178.31	177.46	178.13	177.5	178.31
Multi-mapping reads										
Number of reads mapped to multiple loci	445 740	473 020	417 670	583 207	604 357	643 457	573 357	429 427	515 954	474 032
% of reads mapped to multiple loci	1.94%	1.91%	1.90%	2.05%	2.18%	2.04%	2.00%	1.96%	1.95%	1.99%
Identified transcripts										
Number of identified transcripts	34 613	34 007	34 932	35 935	35 175	36 654	32 931	34 256	33 618	36 026
% of identified transcripts	75.19%	73.87%	75.88%	78.06%	76.41%	79.62%	71.53%	74.41%	73.03%	78.26%

OP — ovaries from 4-*tert*-octyphenol-treated piglets, CTR — ovaries from vehicle (corn oil)-treated piglets.
Each biological sample was sequenced two times (for details please see the M&M section), technical samples: CTR1a and CTR1b, OP1a and OP1b etc.
The statistics are presented for each sample separately.
Preprocessing of data included clipping of adapters, trimming of read ends and removing low quality reads.
"Unique reads" refer to reads that were mapped to a unique (only one) location of the reference genome.
"Multi-mapping reads" refer to reads aligned to more than one locus on the reference genome.
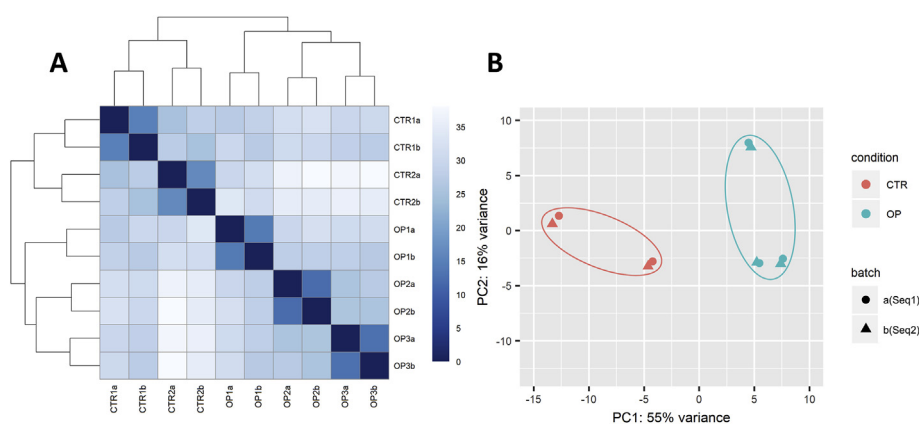

Fig. 1. Distance matrix (A) and PCA plot (B) illustrating the transcriptomic profile of the ovaries collected from pig neonates treated with 4-*tert*-octylphenol (OP). A) The color scale represents the distances between biological replicates, where the most dark blue stands for the smallest distance. B) The plots show results obtained from the analysis performed on four control and six OP-treated piglets, where each piglet represents a biological sample. Each biological sample is represented by two technical replicates (a = Seq1; b = Seq2). . (For interpretation of the references to color in this figure legend, the reader is referred to the Web version of this article.)

study, we focused on one of the most important aspects of ovarian physiology — steroid hormone production. Within the ovarian steroidogenesis signalling pathway we identified three genes which expression was up-regulated after 4-*tert*-octylphenol treatment (Fig. 4B). These were: PLA2 (*PLA2G4E*; phospholipase A2 group IVE; $\log_2$FC: 1.4821), CYP11A (*CYP11A1*; cytochrome P450, family 11, subfamily A, polypeptide 1; $\log_2$FC: 2.6820) and 17β-HSD (*HSD17B2*; hydroxysteroid 17-beta dehydrogenase 2; $\log_2$FC: 1.1782).

To further inquire into the role of DEGs in the ovarian response to 4-*tert*-octylphenol, we analyzed these genes by means of STRING v11.0 tool (https://version-11-0.string-db.org/cgi/network.pl?networkId=Faaxc59PLsDs). The analysis generated a gene/protein interaction network (Fig. 5; the strength of interaction score >0.7) consisting of 40 DEGs (nodes) and 50 edges. Nodes devoid of any interactions were deleted from the network. Four DEGs were classified into "molecular function" (red color) and seven genes were annotated to "cellular component" (green color). *C3* (complement 3, 10 edges), *SERPINA1* (serpin family A member 1, 5 edges), *ALB* (albumin, 5 edges) *F5* (coagulation factor V, 5 edges), *AHSG* (alpha 2-HS glycoprotein, 5 edges), and *ENSSSCG00000009565* (growth arrest specific 6, 5

edges) were the most interacting nodes. The strongest interactions (expressed as the number of links found between any two genes) were identified between: 1/*COL9A1* (collagen type IX alpha 2 chain) and *COL9A2* (collagen type IX alpha 2 chain), 2/*ATP6V1D* (ATPase, H+ transporting, lysosomal 34 kDa, V1 subunit D) and *ATPV1B1* (ATPase H+ transporting V1 subunit B1), and 3/*KERA* (keratocan) and *LUM* (lumican) (Fig. 5).

3.3. Identification of lncRNAs in the ovarian transcriptome of porcine neonates treated with 4-tert-octylphenol

The customized multi-step identification pipeline was applied to distinguish lncRNAs from all assembled transcripts (Fig. 6). A total of 4669 RNA sequences were identified as lncRNAs, including 1236 lncRNAs (located in 355 long non-coding loci) already annotated in databases.

3.4. The effects of 4-tert-octylphenol on the lncRNA expression profile in the ovaries of porcine neonates

A total of 23 differentially expressed lncRNAs (DELs; P-adjusted <0.05; $\log_2$FC $\leq$ 1) were identified in the current study (see
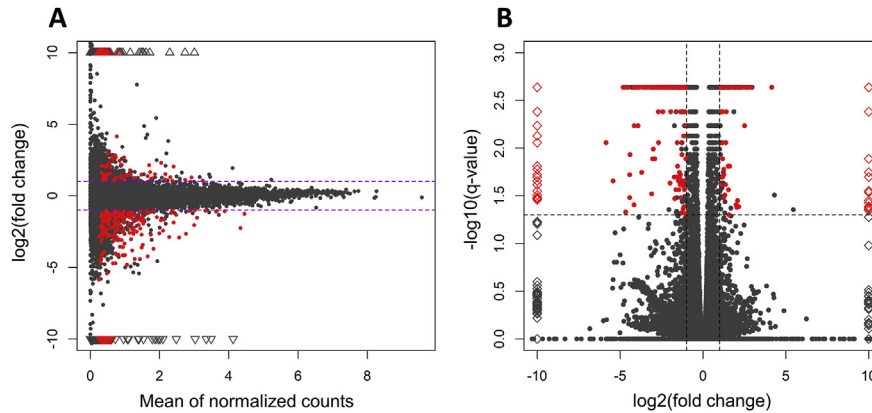
Fig. 2. Distribution of transcripts presented as MA plot (A) and Volcano plot (B) determined by Cufflinks. Red points represent differentially expressed genes (DEGs; P-adjusted < 0.05). Triangles (A) and diamonds (B) represent transcripts with the expression level out of the plot scale. Horizontal lines in the MA plot and vertical lines in the Volcano plot indicate the thresholds of $log_2FC = 1$ and $log_2FC = −1$.. (For interpretation of the references to color in this figure legend, the reader is referred to the Web version of this article.)

Supplementary Table 3). The log_2FC values for DELs ranged from −4.82 (XLOC_006469) to 4.15 (XLOC_018 594). Ten out of 23 DELs identified in the ovaries were up- and 13 were down-regulated. The correlations found between 203 DEGs and 23 DELs identified in the ovaries of pig neonates treated with 4-*tert*-octylphenol are depicted in Supplementary Table 1 and visualized in a form of heatmap in Supplementary Fig. 1. The correlations between two exemplary DEGs (*SERPINA1* and *CYP11A1*) and DELs were found to be only positive; their graphical illustration is shown in Fig. 7 and the corresponding values are presented in Supplementary Table 4.

3.5. The expression of selected genes verified by qRT-PCR

To verify the reliability of the RNA-Seq data, four DEGs, *i.e.*,

claudin 1 (*CLDN1*), cytochrome P450 11A1 (*CYP11A1*), serpin A1 (*SERPINA1*), and serpin A6 (*SERPINA6*) as well as one DEL (TCONS_00036 806) were chosen for qRT-PCR analysis. These transcripts were selected based on their potential importance for the ovarian functions and high log_2FC values. The gene expression patterns obtained by qRT-PCR entirely confirmed the RNA-Seq results (Fig. 8).

4. Discussion

Our recent results supported the hypothesis that neonatal window is critical for programming of the ovarian function. We also showed that androgens and estrogens are important for the assembly of ovarian follicles and their further development in the
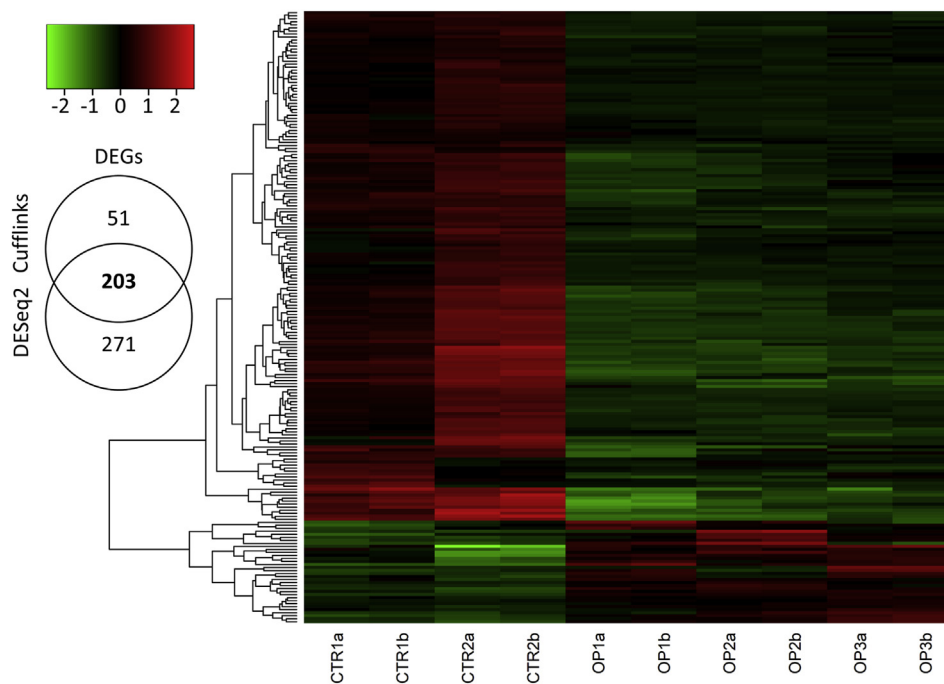

Fig. 3. Differentially expressed genes (DEGs; P-adjusted < 0.05 and log_2 fold change ≥ 1.0) in the ovaries of the 4-*tert*-octylphenol(OP)-treated pig neonates. The left panel presents the number of all differentially expressed genes (DEGs) obtained by employing two statistical methods: Cufflinks and DESeq. The right panel shows a heatmap illustrating the expression profile of all 203 DEGs: the red blocks represent up-regulated genes, and the green blocks represent down-regulated genes; the color scale of the heatmap represents the DEG expression level. . (For interpretation of the references to color in this figure legend, the reader is referred to the Web version of this article.)
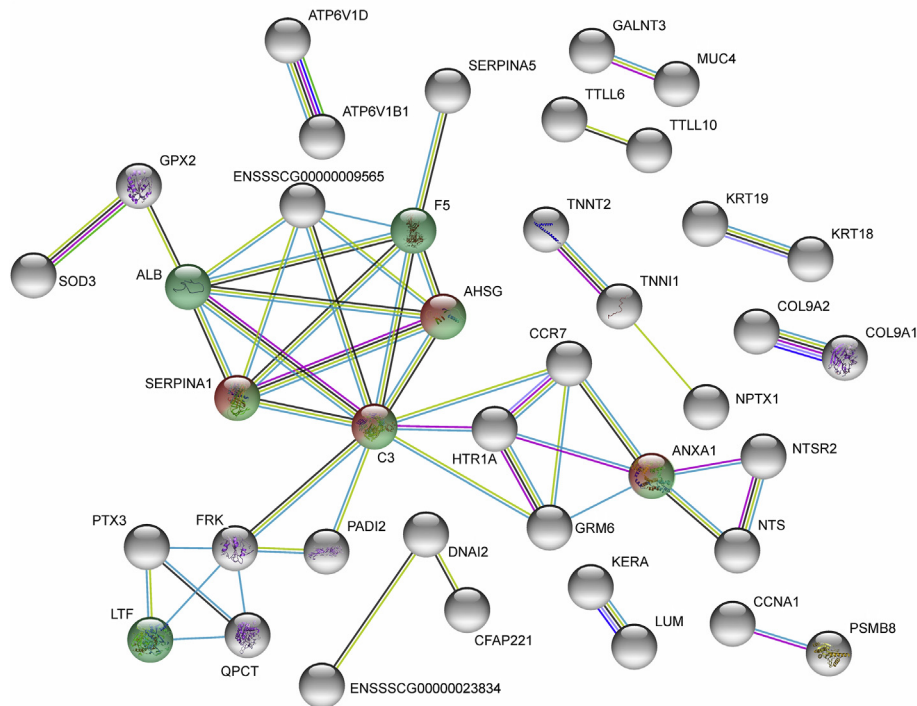
A

B

Fig. 5. STRING-generated interaction network of the differentially expressed genes (DEGs of FC > 2) in the porcine ovaries of 4-*tert*-octylphenol-treated porcine neonates. STRING v11.0 was used to derive the network of 203 DEGs by applying the following prediction methods: text mining (connecting green links), co-expression (connecting black links), experimentally observed interactions (connecting red links) and protein homology (connecting blue links). The nodes that did not interact with other nodes were deleted. The color of the nodes illustrate the assignment to the appropriate GO categories: red — molecular function and green — cellular component. . (For interpretation of the references to color in this figure legend, the reader is referred to the Web version of this article.)

neonatal ovary of the pig [11,12]. Specifically, we demonstrated that neonatal treatment with OP increased the formation of primordial follicles and their initial recruitment as well as increased the ovarian cell proliferation [11]. We also found that neonatal exposure to OP and other EACs affected the GDF9, BMP15, AMH and FSH signalling systems in the ovaries of adult gilts, suggesting their long-term effects on the ovarian development and function [15,16]. In the current study, we employed RNA-Seq to recognize the molecular mechanisms underlying the OP effects on the neonatal ovary of the pig.

In the present study, 203 genes (34 up-regulated and 169 down-regulated) and 23 lncRNAs (10 up-regulated and 13 down-regulated) were found to be differentially expressed in the ovary of the 11-day-old piglets treated neonatally with OP when compared with controls. GO functional annotation analysis showed that DEGs were mainly involved in "movement of cell or subcellular component", "regulation of plasma membrane bounded cell projection assembly" as well as hydrolase and endopeptidase activity. In addition, STRING analysis demonstrated the strongest interactions between SERPINA1, SERPINA5 and AHSG (known as fetuin A), i.e., genes related to negative regulation of endopeptidase activity. In the current study, we observed the up-regulation of SERPINA5 and SERPINA6 expression and the down-regulation of SERPINA1 and SERPINB5 expression in the ovaries of OP-treated pigs. The same effects were generated previously in piglet ovaries by antiandrogen (flutamide) treatment [12]. Serpins are the largest

family of endogenous protease inhibitors which counteract the protease activity and play a role in diverse biological processes including cellular differentiation, apoptosis, fibrinolysis, coagulation, inflammation and cell mobility [30]. The anti-apoptotic function of SERPINA5 has been shown in bovine follicles [31]. Moreover, the up-regulation of *AHSG* expression, which was reported to increase ovarian follicle survival and to promote their growth in rhesus monkey [32], was observed in response to OP treatment. It is suggested that the promotion of primordial follicle formation and cell proliferation induced by OP in piglet ovaries [11] may be associated with the altered expression of serine protease inhibitors.

SERPINA1 was earlier reported to disturb intracellular cholesterol homeostasis in HepG2 cells [33] which may suggest its role in steroidogenesis. In the present study, three up-regulated DEGs (*CYP11A1*, *HSD17B2*, *PLA2*) were enriched in the KEGG ovarian steroidogenesis pathway. Previously we have found that the neonatal antiandrogen-treatment increased the expression of *CYP11A1* — an enzyme related to an initial step in steroidogenesis — in the ovary of 11-day-old piglets [12]. Similarly, it was also demonstrated that other environmental estrogen, methylparaben, increased the *CYP11A1* mRNA level in ovaries of adult rats [34]. On the other hand, a decreased expression of *CYP11A1* was detected in adult mouse testes exposed prenatally to OP [35] and rat ovaries exposed neonatally to parabens [36]. The dose-dependent regulation of *CYP11A1* expression in neonatal rat ovaries has been suggested: the

Fig. 4. A) Gene Ontology (GO) analysis of 203 differentially expressed genes (DEGs) identified in the ovaries of the 4-*tert*-octylphenol (OP)-treated pig neonates. DEGs were classified into three categories of the GO classification (light grey — biological processes, black — molecular functions and dark grey — cellular components), and the number of DEGs is presented over bars. B) Kyoto Encyclopedia of Genes and Genomes (KEGG) analysis of OP-affected DEGs identified in the ovaries of pig neonates and assigned to the ovarian steroidogenesis pathway. The color scale represents the gene expression level, where the most bright green stands for $\log_2$ fold change of -1 and the most bright red stands for $\log_2$ fold change of 1. . (For interpretation of the references to color in this figure legend, the reader is referred to the Web version of this article.)
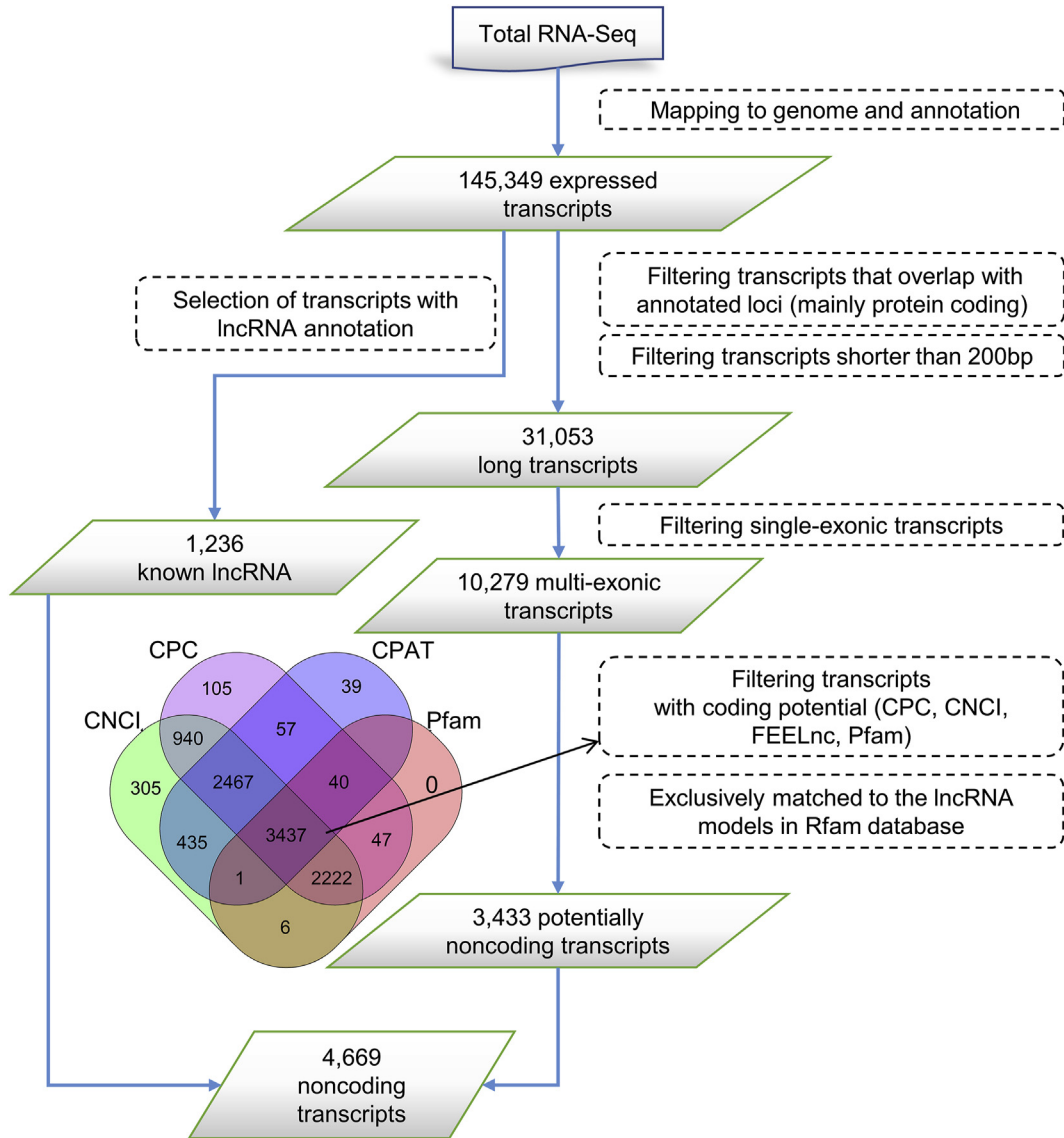
Fig. 6. An overview of the stringent filtering pipeline used to identify 4669 lncRNAs. Rhombic boxes contain the numbers of transcripts (TCONs) that passed a respective filter. Dashed boxes describe actions that were employed at each step of the filtering procedure. Venn diagram shows the number of lncRNAs obtained by using four different tools (CNCI, CPC, CPAT, Pfam) to filter out transcripts with coding potential.
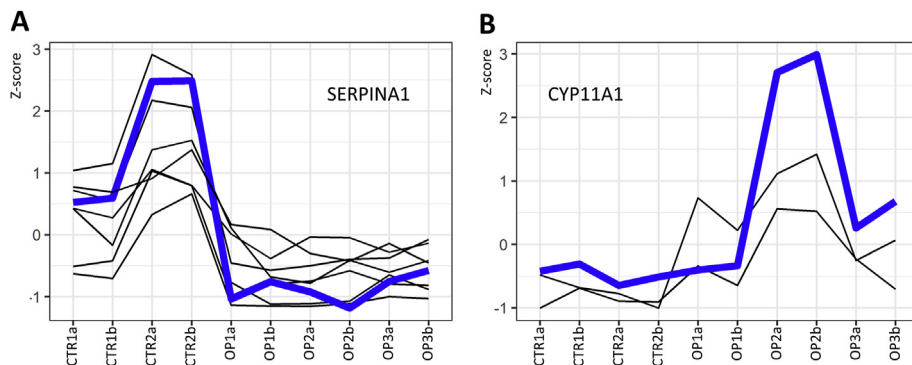

Fig. 7. The effects of correlation analysis performed between two exemplary differentially expressed genes (DEGs; A/SERPINA1, and B/CYP11A1) and differentially expressed lncRNAs (DELs). The expression of DEGs was analyzed in the ovaries of 4-*tert*-octylphenol (OP)-treated porcine neonates by Bioconductor in R package. Expression data are presented as normalized values (Z-scores). The analyzed DEGs are depicted as blue lines and the correlated DELs as black lines. . (For interpretation of the references to color in this figure legend, the reader is referred to the Web version of this article.)
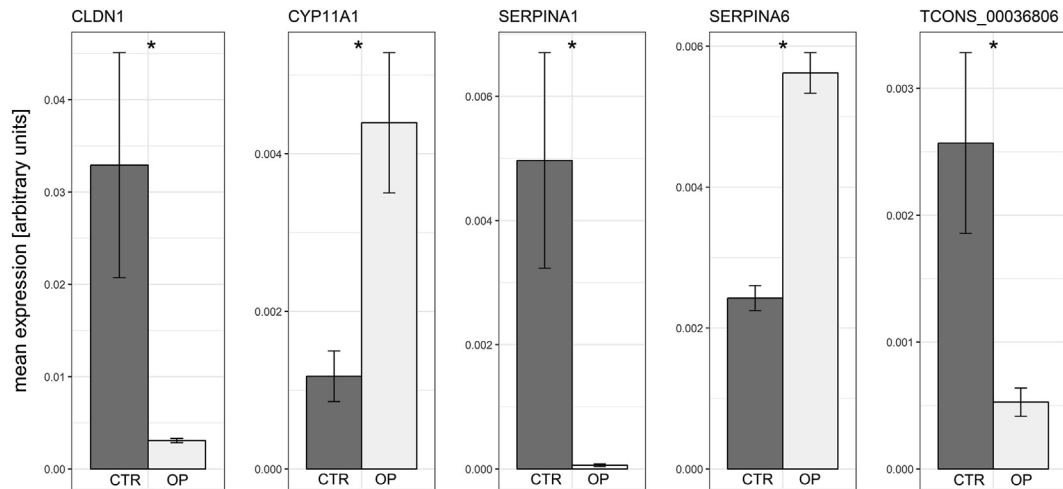
Fig. 8. The results of quantitative real-time PCR of the selected differentially expressed genes (DEGs) and the lncRNA (DEL) identified by RNA-Seq in the ovaries from control (dark grey bars) and 4-*tert*-octylphenol (OP)-treated (light grey bars) neonatal pigs. The validation was performed using the same RNA samples as were used in RNA-Seq. The expression of the selected up- and down-regulated DEGs was presented relatively to GAPDH as mean ± SEM. Asterisks designate significant differences between control (CTR) and OP-treated piglets (Mann-Whitney *U* test; *P < 0.05).
CLDN1: Claudin-1, CYP11A1: cytochrome P450 11A1, SERPINA1: serpin A1, SERPINA6: serpin A6.

gene expression would be positively regulated by low doses and negatively regulated by high doses of estrogenic compounds [36]. It should be also emphasized that, in the current study, the expression of *SERPINA1, CYP11A1, HSD17B2*, and *PLA2G4E* was found to be positively or negatively correlated with the expression of DELs. All these results support the thesis that the neonatal exposure to OP influences ovarian steroid production which may adversely affect reproductive processes in adult life. Moreover, the OP action on the ovary may be partially executed *via* the changes in the lncRNA expression.

Some of the down-regulated DEGs may be involved in the regulation of intracellular transport in ovarian cells of neonatal pigs. Microtubules are multifunctional dynamic protein filaments involved in a variety of important cellular processes, including cell division, development, motility, and intracellular organization. The dynamic nature of microtubules is fundamental to their function and tightly regulated by microtubule-associated proteins [37]. Tubulin tyrosine ligase (TTL) and multiple TTL-like (TTLL) enzymes catalyzing the addition of tyrosine, glutamate or glycine to the tubulin tails have been identified among such proteins [38]. The TTL suppression was linked to cell transformation and correlated with poor prognosis in patients suffering from diverse forms of cancers [39]. Moreover, differential tubulin tyrosination can also affect the behavior of motor proteins and thus intracellular trafficking [40]. In the current study, the expression of *TTLL6, TTLL10* and *KIF19* (kinesin family member 19) was found to be down-regulated in the ovaries of 11-day-old piglets exposed to OP during the neonatal period. In addition, dynein-related genes such as *DNAI2* (dynein axonemal intermediate chain 2), *DRC1* (dynein regulatory complex subunit 1), *DRC7*, and *DYNLRB2* (dynein light chain roadblock-type 2) were also down-regulated. In mammalian cells, cytoplasmic dynein was reported to assist in assembling microtubules into the spindle during cell division as well as to drive intracellular transport towards the minus ends of microtubules [41]. Given that dyneins and kinesins both move along microtubules, we suggest that the OP-induced down-regulation of microtubule-, kinesin- and dynein-associated gene expression in the ovaries of piglets may affect intracellular transport. This may have subsequent implications for ovarian cell physiology, including steroidogenesis, proliferation, and apoptosis [42].

It is well known that membrane transport proteins, including channels and transporters, play a fundamental role in cell functions. It was demonstrated that solute carrier family (SLC) proteins are involved in transporting various molecules across the membranes of the oocyte and cumulus cells in mice [43]. In the current study, OP decreased the expression of the SLC family members, i.e. *SLC2A5, SLC7A11, SLC28A3* and *SLC34A2*. The proteins transport diverse solutes such as glucose, amino acids, nucleosides and lipids, as well as inorganic phosphate across biological membranes [44]. Moreover, voltage-gated potassium channels (*KCNK1* and *KCNJ5*) and potassium channel regulator (*KCNRG*) were differentially expressed in the ovaries of 11-day-old piglets exposed to OP during the neonatal period. The role of potassium channels in cell cycle and proliferation, cell migration, invasion and apoptosis has been previously reported [45]. In addition, the expression of plasma membrane Ca^{2+}-ATPases (PMCAs) involved in the maintenance of Ca^{2+} homeostasis within the cell is crucial for supporting and controlling many cellular and physiological processes [46]. In the present study, we found that neonatal OP treatment down-regulated the expression of PMCA2 (encoded by *ATP2B2*) in ovaries of 11-day-old piglets. All these results suggest that OP-evoked disruption of ovarian development in neonatal pigs might be also associated with changes in the expression of genes involved in membrane transport.

5. Conclusions

The results of the current study extended our knowledge concerning the OP effects on neonatal ovaries of the pig. Recently, we reported the adverse effects of neonatal OP-treatment on the recruitment and growth of primordial follicles [11]. Here, the RNA-Seq approach allowed for detection of OP-induced changes in the ovarian transcriptomic profile of neonatal piglets. OP was found to affect the expression of genes: i) encoding serine protease inhibitors, ii) involved in steroid synthesis and iii) associated with intracellular and membrane transport. It is possible that some of the OP effects on the ovary may be partially executed by an altered lncRNA expression. We suggest that the DEGs identified in the ovaries of OP-treated piglets may disturb ovarian cellular function, including steroidogenesis, proliferation and apoptosis. The disturbances can further

lead to impaired folliculogenesis in the neonatal ovary and may affect female reproduction in adulthood.

Acknowledgements

Appendix A. Supplementary data

Supplementary data to this article can be found online at https://doi.org/10.1016/j.theriogenology.2020.04.027.

References

[1] Monniaux D, Clément F, Dalbiès-Tran R, Estienne A, Fabre S, Mansanet C, et al. The ovarian reserve of primordial follicles and the dynamic reserve of antral growing follicles: what is the link? Biol Reprod 2014;90:85.

[2] Regan SL, Knight PG, Yovich JL, Stanger JD, Leung Y, Arfuso F, et al. Infertility and ovarian follicle reserve depletion are associated with dysregulation of the FSH and LH receptor density in human antral follicles. Mol Cell Endocrinol 2017;446:40—51.

[3] Drummond AE. The role of steroids in follicular growth. Reprod Biol Endocrinol 2006;4:16.

[4] Sweeney T. Is exposure to endocrine disrupting compounds during fetal/postnatal development affecting the reproductive potential of farm animals? Domest Anim Endocrinol 2002;23:203—9.

[5] Uzumcu M, Zachow R. Developmental exposure to environmental endocrine disruptors: consequences within the ovary and on female reproductive function. Reprod Toxicol 2007;23:337—52.

[6] Peterson RE, Cooke PS, Kelce WR, Gray Jr E. Environmental endocrine disruptors. In: Sipes IG, McQueen CA, Gandolfi AJ, editors. Comprehensive toxicology, vol. 10. Cambridge: Elsevier; 1997. p. 181—92.

[7] Bøgh IB, Christensen P, Dantzer V, Groot M, Thøfner IC, Rasmussen RK, et al. Endocrine disrupting compounds: effect of octylphenol on reproduction over three generations. Theriogenology 2001;55:131—50.

[8] White R, Jobling S, Hoare S, Sumpter J, Parker M. Environmentally persistent alkylphenolic compounds are estrogenic. Endocrinology 1994;135:178—82.

[9] Aydoğan M, Barlas N. Effects of maternal 4-tert-octylphenol exposure on the reproductive tract of male rats at adulthood. Reprod Toxicol 2006;22:455—60.

[10] Katsuda S, Yoshida M, Watanabe G, Taya K, Maekawa A. Irreversible effects of neonatal exposure to p-tert-octylphenol on the reproductive tract in female rats. Toxicol Appl Pharmacol 2000;165:217—26.

[11] Knapczyk-Stwora K, Grzesiak M, Cierszko RE, Czaja E, Koziorowski M, Slomczynska M. The impact of sex steroid agonists and antagonists on folliculogenesis in the neonatal porcine ovary via cell proliferation and apoptosis. Theriogenology 2018;113:19—26.

[12] Knapczyk-Stwora K, Nynca A, Cierszko RE, Paukszto L, Jastrzebski JP, Czaja E, et al. Flutamide-induced alterations in transcriptional profiling of neonatal porcine ovaries. J Anim Sci Biotechnol 2019;10:35.

[13] Rinn JL, Chang HY. Genome regulation by long noncoding RNAs. Annu Rev Biochem 2012;81:145—66.

[14] Dykes IM, Emanueli C. Transcriptional and post-transcriptional gene regulation by long non-coding RNA. Dev Reprod Biol 2017;5:177—86.

[15] Knapczyk-Stwora K, Grzesiak M, Witek P, Duda M, Koziorowski M, Slomczynska M. Neonatal exposure to agonists and antagonists of sex steroid receptors induces changes in the expression of oocyte-derived growth factors and their receptors in ovarian follicles in gilts. Theriogenology 2019;134:42—52.

[16] Knapczyk-Stwora K, Grzesiak M, Witek P, Duda M, Koziorowski M, Slomczynska M. Neonatal exposure to agonists and antagonists of sex steroid receptors affects AMH and FSH plasma level and their receptors expression in the adult pig ovary. Animals (Basel) 2020;10:12.

[17] Myllymäki SA, Karjalainen M, Haavisto TE, Toppari J, Paranko J. Infantile 4-tert-octylphenol exposure transiently inhibits rat ovarian steroidogenesis and steroidogenic acute regulatory protein (StAR) expression. Toxicol Appl Pharmacol 2005;207(1):59—68.

[18] Bolger AM, Lohse M, Usadel B. Trimmomatic: a flexible trimmer for Illumina sequence data. Bioinformatics 2014;30:2114—20.

[19] Dobin A, Davis CA, Schlesinger F, Drenkow J, Zaleski C, Jha S, et al. STAR: ultrafast universal RNA-seq aligner. Bioinformatics 2013;29:15—21.

[20] Pertea M, Pertea GM, Antonescu CM, Chang TC, Mendell JT, Salzberg SL. StringTie enables improved reconstruction of a transcriptome from RNA-seq reads. Nat Biotechnol 2015;33:290—5.

[21] Pertea M, Kim D, Pertea GM, Leek JT, Salzberg SL. Transcript-level expression analysis of RNA-seq experiments with HISAT, StringTie and Ballgown. Nat Protoc 2016;11:1650—67.

[22] Trapnell C, Roberts A, Goff L, Pertea G, Kim D, Kelley DR, et al. Differential gene and transcript expression analysis of RNA-seq experiments with TopHat and cufflinks. Nat Protoc 2012;7:562—78.

[23] Love MI, Huber W, Anders S. Moderated estimation of fold change and dispersion for RNA-seq data with DESeq2. Genome Biol 2014;15:550.

[24] Gentleman RC, Carey VJ, Bates DM, Bolstad B, Dettling M, Dudoit S, et al. Bioconductor: open software development for computational biology and bioinformatics. Genome Biol 2004;5:R80.

[25] Huber W, Carey VJ, Gentleman R, Anders S, Carlson M, Carvalho BS, et al. Orchestrating high-throughput genomic analysis with Bioconductor. Nat Methods 2015;12:115—21.

[26] Reimand J, Arak T, Adler P, Kolberg L, Reisberg S, Peterson H, et al. profiler-a web server for functional interpretation of gene lists (2016 update). Nucleic Acids Res 2016;44:W83—9.

[27] Snel B, Lehmann G, Bork P, Huynen MA. STRING: a web-server to retrieve and display the repeatedly occurring neighbourhood of a gene. Nucleic Acids Res 2000;28:3442—4.

[28] Ruszkowska M, Nynca A, Paukszto L, Sadowska A, Swigonska S, Orlowska K, et al. Identification and characterization of long non-coding RNAs in porcine granulosa cells exposed to 2,3,7,8-tetrachlorodibenzo-p-dioxin. J Anim Sci Biotechnol 2018;9:72.

[29] Zhao S, Fernald RD. Comprehensive algorithm for quantitative real-time polymerase chain reaction. J Comput Biol 2005;12:1047—64.

[30] Law RH, Zhang Q, McGowan S, Buckle AM, Silverman GA, Wong W, et al. An overview of the serpin superfamily. Genome Biol 2006;7:216.

[31] Hayashi KG, Ushizawa K, Hosoe M, Takahashi T. Differential gene expression of serine protease inhibitors in bovine ovarian follicle: possible involvement in follicular growth and atresia. Reprod Biol Endocrinol 2011;9:72.

[32] Xu J, Lawson MS, Yeoman RR, Pau KY, Barrett SL, Zelinski MB, et al. Secondary follicle growth and oocyte maturation during encapsulated three-dimensional culture in rhesus monkeys: effects of gonadotropins, oxygen and fetuin. Hum Reprod 2011;26:1061—72.

[33] Janciauskiene S, Lindgren S, Wright HT. The C-terminal peptide of alpha-1-antitrypsin increases low density lipoprotein binding in HepG2 cells. Eur J Biochem 1998;254:460—7.

[34] Lee JH, Lee M, Ahn C, Kang HY, Tran DN, Jeung EB. Parabens accelerate ovarian dysfunction in a 4-vinylcyclohexene diepoxide-induced ovarian failure model. Int J Environ Res Publ Health 2017;14:E161.

[35] Buñay J, Larriba E, Patiño-Garcia D, Cruz-Fernandes L, Castañeda-Zegarra S, Rodriguez-Fernandez M, et al. Editor's Highlight: differential effects of exposure to single versus a mixture of endocrine-disrupting chemicals on steroidogenesis pathway in mouse testes. Toxicol Sci 2018;161:76—86.

[36] Ahn HJ, An BS, Jung EM, Yang H, Choi KC, Jeung EB. Parabens inhibit the early phase of folliculogenesis and steroidogenesis in the ovaries of neonatal rats. Mol Reprod Dev 2012;79:626—36.

[37] Howard J, Hyman AA. Dynamics and mechanics of the microtubule plus end. Nature 2003;422:753—8.

[38] Yu I, Garnham CP, Roll-Mecak A. Writing and reading the tubulin code. J Biol Chem 2015;290:17163—72.

[39] Whipple RA, Matrone MA, Cho EH, Balzer EM, Vitolo MI, Yoon JR, et al. Epithelial-to-mesenchymal transition promotes tubulin detyrosination and microtentacles that enhance endothelial engagement. Canc Res 2010;70:8127—37.

[40] Konishi Y, Setou M. Tubulin tyrosination navigates the kinesin-1 motor domain to axons. Nat Neurosci 2009;12:559—67.

[41] Roberts AJ, Kon T, Knight PJ, Sutoh K, Burgess SA. Functions and mechanics of dynein motor proteins. Nat Rev Mol Cell Biol 2013;14:713—26.

[42] Li B, Dou SX, Yuan JW, Liu YR, Li W, Ye F, et al. Intracellular transport is accelerated in early apoptotic cells. Proc Natl Acad Sci USA 2018;115:12118—23.

[43] Wang S, Kou Z, Jing Z, Zhang Y, Guo X, Dong M, et al. Proteome of mouse oocytes at different developmental stages. Proc Natl Acad Sci USA 2010;107:17639—44.

[44] Hediger MA, Romero MF, Peng JB, Rolfs A, Takanaga H, Bruford EA. The ABCs of solute carriers: physiological, pathological and therapeutic implications of human membrane transport proteinsIntroduction. Pflügers Archiv 2004;447:465—8.

[45] Pardo LA, Stühmer W. The roles of K(+) channels in cancer. Nat Rev Canc 2014;14:39—48.

[46] Monteith GR, Roufogalis BD. The plasma membrane calcium pump-a physiological perspective on its regulation. Cell Calcium 1995;18:459—70.